

The role of Er^{3+} – Er^{3+} separation on the luminescence of Er-doped Al_2O_3 films prepared by pulsed laser deposition

R. Serna,^{a)} M. Jiménez de Castro, J. A. Chaos, and C. N. Afonso
Instituto de Optica, C.S.I.C., Serrano 121, 28006 Madrid, Spain

I. Vickridge
GPS, Universités Paris VI et VII, UMR7588, Tour 23 2, Place Jussieu, 75251-Paris Cedex 5, France

(Received 21 June 1999; accepted for publication 4 November 1999)

Erbium-doped Al_2O_3 films have been deposited in a single step process by pulsed laser deposition using independent ablation of Al_2O_3 and Er targets. This procedure allows to control the Er^{3+} ions in-depth distribution. The characteristic Er^{3+} photoluminescence at $1.54 \mu\text{m}$ shows lifetime values which increase from 6.0 to 7.1 ms when the Er^{3+} – Er^{3+} in-depth separation is increased from 3 to 9 nm. These results are discussed in terms of the ion–ion interaction and clustering for separations shorter than 6 nm. © 1999 American Institute of Physics. [S0003-6951(99)04952-9]

After the success of the Er-doped fiber amplifier at $1.5 \mu\text{m}$, the Er^{3+} -doped planar optical waveguide amplifier has received great attention as it will be one of the key elements for the development of high performance integrated optical circuits.^{1–3} It has been acknowledged that to achieve a reasonable gain over a length of a few centimeters, and due to the relatively small emission cross section of the first Er^{3+} excited state, the concentration of optically active Er^{3+} ions has to be in the $10^{20} \text{ ions cm}^{-3}$ range.^{2–4} The interaction between Er^{3+} ions becomes an important gain-limiting effect at such high Er^{3+} concentrations, since the Er^{3+} – Er^{3+} separation will be of the order of a few nanometers, and closely spaced Er^{3+} ions show concentration quenching effects which deteriorate the amplifier performance,^{1,3,4} such as energy migration and cooperative upconversion (also called cross relaxation). Both effects depend partially on the nature of the host material and moreover, they depend strongly on the so-called microscopic distribution of the Er^{3+} ions in the host material. Recently, it has been shown that in order to achieve efficient amplification it is essential to optimize the preparation method to obtain an homogeneous Er^{3+} ion distribution.⁵

We have shown that pulsed laser deposition (PLD) is a suitable method to produce Er^{3+} -doped glasses⁶ and Al_2O_3 ^{7,8} thin films. In this letter, taking advantage of the capability of alternate PLD from two separate targets to control the Er^{3+} ions in-depth separation, we aim to investigate the influence of this separation on the photoluminescence (PL) intensity and lifetime. Such a study has not been pursued before since most studies of rare-earth doping by thin film deposition techniques (PLD,^{9,10} sputtering^{11,12}) have been carried out using a single Er^{3+} -doped target.

The thin films were deposited in vacuum (10^{-7} Torr) using an ArF excimer laser ($\lambda = 193 \text{ nm}$, $\tau = 12 \text{ ns}$ full width at half maximum, 5 Hz repetition rate) with an energy density of approximately 2 J cm^{-2} . The targets were placed in a computer-controlled holder which allows us to alternately ablate the Al_2O_3 and the Er targets.^{7,8} Chemically cleaned Si

(100) wafers held at room temperature were used as substrates. The Er/ Al_2O_3 deposition was repeated a number of times (cycles), alternating one pulse on the Er target with a number of pulses on the Al_2O_3 target which was varied in order to change the Er depth profile while keeping a constant film thickness. Table I includes the relevant deposition parameters. The film thickness was controlled by *in situ* reflectivity measurements.¹³ From the structural point of view, transmission electron microscopy analysis shows that the as-deposited Al_2O_3 films are amorphous.^{13,14}

The Er content and concentration depth profile were measured by Rutherford backscattering spectrometry (RBS) using a 2.0 MeV He^+ beam and a scattering angle of 165° . Figure 1 shows a typical RBS spectrum obtained from the 100 cycle film. Although the individual Er deposits are not resolved, the Er profile from channel 407 to 474 is fairly flat, showing that an even depth distribution has been achieved. The data obtained from the RBS analyses are summarized in Table I. An areal density in the range of $10^{13} \text{ Er atoms cm}^{-2}$ is deposited per pulse. This is equivalent to a submonolayer coverage of Er on the Al_2O_3 surface, which is subsequently buried by the following Al_2O_3 deposition. It is worth noting that alternate PLD at room temperature has been successfully used to deposit well defined layers of metal clusters (Cu, Fe, Bi)^{13–15} separated by Al_2O_3 , indicating that, once the material is deposited on the surface, the metal atoms remain in the

TABLE I. Parameters used in the film deposition, areal densities of Al_2O_3 and Er determined from RBS analysis, and Er areal density per layer calculated by dividing the total Er areal density by the number of deposit cycles. The total thickness of the films is $300 \pm 10 \text{ nm}$ assuming the density of amorphous Al_2O_3 given in Ref. 15.

Deposition parameters		RBS analysis		
No. of cycles	No. pulses on Al_2O_3 per cycle	Al_2O_3 ($\times 10^{18} \text{ cm}^{-2}$)	Er ($\times 10^{15} \text{ cm}^{-2}$)	Er per layer ($\times 10^{13} \text{ cm}^{-2}$)
100	278	2.70 ± 0.05	3.5 ± 0.1	3.5 ± 0.1
50	556	2.70 ± 0.05	2.3 ± 0.1	4.6 ± 0.1
33	834	2.55 ± 0.05	1.5 ± 0.1	4.5 ± 0.1

^{a)}Electronic mail: rserna@io.cfmac.csic.es

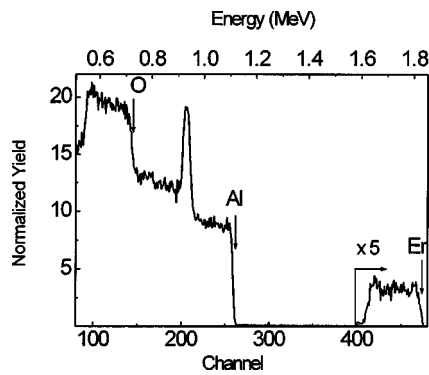


FIG. 1. RBS spectrum for the as-deposited 100 cycles film on Si. The peak around channel 206 is due to the superposition of the signal from the Al_2O_3 film and the Si signal from the underlying substrate. Surface channel of the different elements are indicated on the figure.

film plane and they are not affected by the subsequent Al_2O_3 deposition. This is in contrast to the Er surface segregation observed when doping crystalline materials during growth, as for example Er doping of Si by molecular beam epitaxy.¹⁶ The separation between the Er submonolayers can be calculated by dividing the total measured Al_2O_3 thickness by the number of cycles used to grow the films and it is 3, 6, and 9 nm for the 100, 50, and 33 cycles films, respectively. Note that the Er is distributed in discrete layers in which the local concentration of Er is high. The *average* Er concentration in the film can be estimated from the data on Table I and it is between $1 \times 10^{20} \text{Er cm}^{-3}$ (33 cycles film) and $5 \times 10^{19} \text{Er cm}^{-3}$ (100 cycles film).

PL measurements were performed at room temperature using a monochromator and a liquid-nitrogen cooled Ge detector. The 514.5 nm line of an Ar^+ ion laser (pump power 140 mW) was used as the excitation source, the incident beam forming an angle of 25° with the sample normal.⁶ The PL spectra for all the as-deposited films show the characteristic peak around $1.54 \mu\text{m}$ with a structure similar to that reported elsewhere for Er-doped Al_2O_3 films grown by PLD.^{7,8} The PL decay was found to be a single exponential for all the cases. In order to improve the luminescence characteristics, postdeposition thermal anneals were performed.⁷ The procedure consisted in annealing each film for 1 h in air at a given temperature, then measure the PL intensity and lifetime, and subsequently perform a new 1 h anneal at a higher temperature. This procedure was repeated up to 900°C in 50°C steps. No significant changes of the Er distribution in the films were observed by RBS upon annealing. This result is in agreement with earlier reports for Er-doped Al_2O_3 by other methods in which no Er diffusion was observed up to 950°C .^{11,17} Damage of the film surface was observed by eye after annealing at 900°C and thus annealings at higher temperatures were not performed. The typical evolution of the PL peak intensity and lifetime with the annealing temperature can be seen in Fig. 2. A gradual increase of both values is observed as the temperature is increased from 650 to 900°C . The fact that the increase in the PL intensity follows in a proportional way the increase in the lifetime indicates that the main process induced upon annealing is a reduction of non-radiative decay channels, as it has already been discussed in an earlier work.⁷ This is quite different to what is found in sputter deposited films in which a

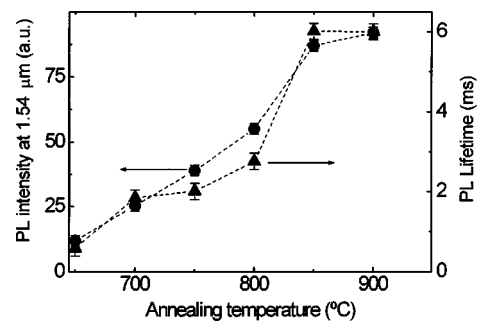


FIG. 2. PL peak intensity at $1.54 \mu\text{m}$ (●) and lifetime (▲) for the 100 cycles Er-doped Al_2O_3 film as a function of the annealing temperature.

low-temperature annealing (500°C) leads to a decrease in the PL intensity which has been explained as a consequence of hydrogen desorption.¹¹

The maximum values for the PL intensity and lifetime are reached after annealing at 850°C . Figure 3 shows these values as a function of the Er^{3+} - Er^{3+} ions in-depth separation. The PL intensity decreases as the Er separation increases, in agreement with the decrease of the total number of Er ions, whereas the lifetime follows the opposite dependence. This effect is more accentuated for Er-Er separations of 3 nm and it is observed at all annealing temperatures. The decrease in lifetime for high average Er concentrations has usually been attributed to an increase in the number of non-radiative decay channels, such as implantation-induced defects in the case of Er implanted samples, or to Er concentration quenching.^{1,2,17} The present results show that the modification of the distance between active Er^{3+} ions *only in one dimension* leads to a significant variation of the lifetime values, this Er^{3+} - Er^{3+} interaction being specially relevant for distances shorter than 6 nm. This result suggests that in this case the lifetime decrease is dominated by concentration quenching.

PL intensity and lifetime are related through rate equations governing the excitation and decay of the Er^{3+} ions. Assuming that pumping with the Ar^+ laser leads to the excitation into the $^2\text{H}_{11/2}$ manifold, which is followed by a rapid decay to the first excited state, the PL intensity corresponding to the transition to the ground state can then be approximated in steady state conditions for a constant pump intensity and at fixed wavelength as

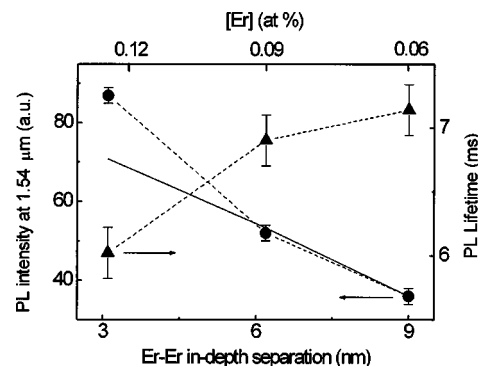


FIG. 3. PL peak intensity (●) and lifetime (▲) as a function of the Er^{3+} - Er^{3+} ion in-depth separation after the 850°C annealing. The *average* Er concentration is quoted for reference at the top axis.

$$I_{\text{PL}} \propto f N \frac{\tau}{\tau_r}, \quad (1)$$

where f is the fraction of active Er^{3+} ions, N the total Er concentration, τ_r the radiative lifetime, and τ the measured lifetime. The measured lifetime is related to the radiative lifetime following the relationship $1/\tau = 1/\tau_r + 1/\tau_{\text{nr}}$, with τ_{nr} being the nonradiative lifetime. As the radiative lifetime τ_r can be considered constant, any nonradiative decay channel leads to a measured lifetime τ less than the radiative lifetime τ_r . Taking into account the experimental lifetime data shown in Fig. 3(b) and the experimental values for N from the RBS data in Table I, the expected PL intensity has been calculated as a function of the Er^{3+} concentration using Eq. (1). The result has been plotted in full line in Fig. 3(a) for an arbitrary constant fraction f of active Er^{3+} ions. There is a good agreement for the low average Er concentration films, indicating that in both cases the fraction of active Er^{3+} ions f is the same. Nevertheless, for the highest average Er concentration film, the expected PL intensity is lower than the experimental values, thus indicating that in this case f is larger. This result can be related to the fact that the areal density of Er^{3+} ions deposited per pulse for the 100 cycles film is 3.5×10^{13} atoms cm^{-2} , 20% less than that deposited in the other two films (4.6×10^{13} atoms cm^{-2} , see Table I). Therefore, the higher f value in this film might be a result of a lesser in-plane clustering and/or of a reduction in Er^{3+} - Er^{3+} ion interaction in the film plane. The average in-plane Er^{3+} - Er^{3+} ion separation can be estimated from the areal Er density determined by RBS and is about 2 nm in our films. It is worth noting that this is an average in-plane distance rather than a real separation distance as the one provided for the direction normal to the film plane.

The present results demonstrate that it is possible to change the PL response by modifying locally the Er^{3+} - Er^{3+} ion interaction. The most likely Er^{3+} - Er^{3+} interaction contributing to the lifetime decrease in the present experimental conditions is excitation migration. By this process some of the excited Er ions transfer their energy to a nearby unexcited Er^{3+} ion, and it becomes detrimental when some of the Er ions are coupled to nonradiative quenching sites. A typical defect found in Er-doped films is the presence of OH complexes whose stretch vibration is resonant with the Er^{3+} transition from the first excited state to the ground state. They have been shown to be responsible for luminescence quenching in materials deposited by thin film techniques such as metalorganic chemical vapor deposition (MOCVD)¹⁸

and sol-gel,¹⁹ but their formation during PLD in vacuum has not yet been investigated.

In summary, Er-doped Al_2O_3 films produced by PLD show Er^{3+} PL lifetimes larger than 6 ms for average concentrations in the order of 10^{20} Er cm^{-3} . The lifetime increases from 6.0 to 7.1 ms when the Er^{3+} - Er^{3+} in-depth separation is increased from 3 to 9 nm, while the Er^{3+} in-plane average separation is kept approximately constant. In the present experimental conditions the Er^{3+} - Er^{3+} interaction that dominates the behavior of the PL lifetime seems to be excitation migration. In addition, it has been found that the fraction of active Er^{3+} ions depends on the Er^{3+} in-plane concentration, this effect being possibly related to some degree of clustering in the film plane.

This work was supported by CICYT (Spain) under TIC96-0467 project and by GDR86 of the CNRS (France). It is a pleasure to acknowledge helpful and encouraging discussions with Dr. J. Solis (Instituto de Optica).

¹J. Smulovich, Proc. SPIE **2996**, 143 (1997).

²Mater. Res. Bull. **23**, 16 (1998).

³A. Polman, J. Appl. Phys. **82**, 1 (1997).

⁴Ch. Buchal, Th. Siegrist, D. C. Jacobson, and J. M. Poate, Appl. Phys. Lett. **68**, 438 (1996).

⁵P. G. Kik and A. Polman, Mater. Res. Bull. **23**, 48 (1998).

⁶R. Serna, J. M. Ballesteros, M. Jiménez de Castro, J. Solís, and C. N. Afonso, J. Appl. Phys. **84**, 2352 (1998).

⁷R. Serna and C. N. Afonso, Appl. Phys. Lett. **69**, 1541 (1996).

⁸R. Serna, C. N. Afonso, J. M. Ballesteros, and A. Zschocke, Appl. Surf. Sci. **109-110**, 524 (1997).

⁹K.-M. Wang, B.-R. Shi, N. Cue, Y.-Y. Zhu, R.-F. Xiao, F. Lu, W. Li, and Y.-G. Liu, Appl. Phys. Lett. **73**, 1020 (1998).

¹⁰K. G. Cho, D. Kumar, P. H. Holloway, and R. K. Singh, Appl. Phys. Lett. **73**, 3058 (1998).

¹¹S. K. Lazarouk, A. V. Mudryi, and V. E. Borisenko, Appl. Phys. Lett. **73**, 2272 (1998).

¹²Y. C. Yan, A. J. Faber, H. De Waal, P. G. Kik, and A. Polman, Appl. Phys. Lett. **71**, 2922 (1997).

¹³C. N. Afonso, R. Serna, J. M. Ballesteros, A. K. Petford-Long, and R. C. Doole, Appl. Surf. Sci. **127-129**, 339 (1998).

¹⁴R. Serna, C. N. Afonso, J. M. Ballesteros, A. Naudon, D. Babonneau, and A. K. Petford-Long, Appl. Surf. Sci. **138-139**, 1 (1999).

¹⁵R. Serna, J. C. G. de Sande, J. M. Ballesteros, and C. N. Afonso, J. Appl. Phys. **84**, 4509 (1998).

¹⁶R. Serna, J. H. Shin, M. Lohmeier, E. Vlieg, A. Polman, and P. F. A. Alkemade, J. Appl. Phys. **79**, 2658 (1996).

¹⁷G. N. van den Hoven, E. Snoeks, A. Polman, J. W. M. van Uffelen, Y. S. Oei, and M. K. Smit, Appl. Phys. Lett. **62**, 3065 (1993).

¹⁸G.-C. Yi, B. A. Block, G. M. Ford, and B. W. Wessels, Appl. Phys. Lett. **73**, 1625 (1998).

¹⁹M. Benatsou, B. Capoen, M. Bouzaoui, W. Tchana, and J. P. Vilcot, Appl. Phys. Lett. **71**, 428 (1997).